

Ultrafast laser fabrication of Bragg waveguides in chalcogenide glass

Ben McMillen, Mingshan Li, Sheng Huang, Botao Zhang, and Kevin P. Chen*

Department of Electrical Engineering, University of Pittsburgh, Pittsburgh, Pennsylvania 15261, USA

*Corresponding author: kchen@engr.pitt.edu

Received March 24, 2014; revised April 23, 2014; accepted May 1, 2014;

posted May 5, 2014 (Doc. ID 208740); published June 10, 2014

Bragg waveguides are fundamental components in photonic integrated circuits and are particularly interesting for mid-IR applications in high index, highly nonlinear materials. In this work, we present Bragg waveguides fabricated in bulk chalcogenide glass using an ultrafast laser. Waveguides with near circularly symmetric cross sections and low propagation loss are obtained through spatial and temporal beam shaping. Using a single-pass technique, the waveguide and Bragg structure are formed at the same time. First through sixth order gratings with strengths of up to 25 dB are realized, and performance is evaluated based on the modulation duty cycle of the writing beam. © 2014 Optical Society of America

OCIS codes: (350.3390) Laser materials processing; (130.2755) Glass waveguides; (160.4330) Nonlinear optical materials.

<http://dx.doi.org/10.1364/OL.39.003579>

Chalcogenide (ChG) glasses are known for their excellent mid-IR transparency and large nonlinear refractive indices of up to 1000 times that of fused silica [1,2]. These unique traits make them attractive in a wide range of applications. In particular, ChG glasses are suitable substrate materials for fabricating photonic integrated circuits (PICs), due to inherently large χ_3 nonlinearities with ultrafast response times and low two-photon absorption at telecom wavelengths. These properties become especially important in applications such as high-data-rate signal processing [3–5]. In such PIC devices, Bragg waveguides are often employed as basic building blocks, enabling operations such as 2R regeneration [6,7], and all-optical switching [8]. Fabrication of these structures generally relies on thin film deposition and various photolithography schemes. However, thin-film processes incur restrictions when building multilayer structures for complex optical interconnects by limiting devices to a planar geometry.

Ultrafast laser writing offers great design flexibility with its capability for making three-dimensional structures [9,10] and is a proven technique to form high-quality waveguides in bulk optical substrates. Extensions of this technology have also been applied to the fabrication of Bragg waveguides in fused silica using several approaches, such as the point-by-point technique [11–13], and the multiscan technique [14]. Applying these methods to ChG glasses, however, presents a unique design challenge. The high refractive index of these materials induces spherical aberrations at the focus of the writing beam, which are further compounded by nonlinear effects brought about by high-intensity laser pulses. These interactions often lead to self-focusing and filamentation, producing highly asymmetrical waveguides with an elongated cross section and multiple guiding regions [15]. Mitigation of these effects is essential for fabricating high-quality waveguides in ChG glasses.

Recently, it has been demonstrated that temporal [16] and spatial beam shaping [17] may be used to control the size and shape of the cross section of a laser-written waveguide. These techniques, combined with adjustment of other processing parameters such as writing speed,

pulse energy, and repetition rate, have produced nearly symmetric waveguides with propagation losses as low as 0.65 dB/cm at 1560 nm [18]. With this exceptionally low propagation loss and precise control over the waveguide cross section, this technique provides a new avenue for fabricating complex optical structures in highly nonlinear materials.

In this Letter, the techniques of temporal and spatial beam shaping are applied to fabrication of low-loss Bragg waveguides in bulk ChG substrates using a single-scan technique. Waveguides with grating strengths of up to 25 dB at a resonant wavelength of ~ 1550 nm are realized by forming multiorder grating structures, with periods ranging from the first (fundamental) to sixth order. Characteristics such as guiding performance and grating response are evaluated with respect to modulation duty cycle, and optimum values are presented which represent the best compromise between grating strength and bandwidth. These process parameters may be applied directly to fabrication of devices for mid-IR applications, whose fundamental Bragg wavelength lies within the range of the multiorder grating waveguides presented here.

The substrate material used in this work is a gallium lanthanum sulfide (GLS) ChG glass ($25 \times 25 \times 1$ mm, ChG Southampton), which was chosen for its high nonlinear figure of merit and superior environmental stability [19]. Laser pulses at a wavelength of 800 nm were produced by a Ti:sapphire regenerative amplifier system (Coherent RegA 9000), delivering a pulse width of 150 fs at a repetition rate of 250 kHz. To mitigate focal distortions, a longer pulse duration of 1.5 ps was used in combination with a cylindrical telescope, providing a demagnification factor of ~ 3 perpendicular to the writing direction. This astigmatic beam shaping tool produces a free-space focal plane offset [17], which allows for full control over the size and shape of the focal volume. The cylindrical telescope produced an elliptical beam, with the major axis oriented along the writing direction, filling the input aperture of an $80\times$ (0.75 NA) microscope objective. The beam was then circularly polarized before being delivered to the ChG substrate with the objective, forming a focus

275 μm beneath the surface. Spatial beam shaping, in combination with longer pulse duration, allows for mitigation of beam distortions at the focus, resulting in a nearly circular waveguide cross section in GLS ChG glass [18]. Moreover, full control over the size and shape of the waveguide cross section is realized by adjusting the distance between the two cylindrical lenses, thereby tuning the astigmatic difference. The technical details of the optical setup used in this work can be found in [17].

Bragg waveguides were fabricated by translating the substrate in relation to a fixed focal position using a three-axis air-bearing stage. A single-scan technique was employed, in which periodic modulation of the writing beam induces a series of partially overlapping refractive index voxels, forming a waveguide and Bragg structure at the same time. The pulse energy and translation speed were fixed at 300 nJ and 1000 $\mu\text{m}/\text{s}$ respectively, providing a reasonable compromise between waveguide shape and minimal nonlinear effects, while still inducing enough fringe contrast to produce strong gratings. The overlapping voxels contain adequate DC index change to support guided modes, while the induced AC index modulation provides the periodic structure required for Bragg reflections. Modulation of the writing beam was achieved by triggering the cavity dumper in the regenerative amplifier using a periodic signal, with the modulation frequency given by $f = 2vn_{\text{eff}}/m\lambda_B$, where m is the grating order, v is the translation speed of the sample, n_{eff} is the effective refractive index of the waveguide core, and λ_B is the Bragg wavelength. Bragg waveguides studied in this work were designed for a center wavelength of $\lambda_B \sim 1550$ nm and $n_{\text{eff}} = 2.37$ with a fixed writing velocity of $v = 1000$ $\mu\text{m}/\text{s}$. Modulation frequencies were chosen to form Bragg waveguides from the first to the sixth order, with grating periods ranging from 0.329 to 1.97 μm . Figure 1 shows a white light microscope image of the multiorder Bragg waveguides as viewed from the incident direction of the writing beam. A zero-order waveguide (no grating) is also shown for comparison. Two

sets of Bragg waveguides were formed with beam modulation duty cycles of 25% and 50%, respectively. In both cases, periodic structures are visible in the second through sixth order gratings, while features in the first-order gratings are beyond the resolution of the optical microscope. The thermal and time stability of these structures was not studied in this work; however, recent publications have shown that structures written under similar conditions in GLS are stable at temperatures up to 235°C [20].

Guiding performance of the waveguides was evaluated by grinding and polishing the end facets of the substrate, followed by coupling 1560 nm CW light into one end of each waveguide via a single-mode fiber. The output facet was then imaged with a 50 \times microscope objective attached to an infrared CCD camera, which provided near field imaging of the guided mode profile. Figure 2 shows a comparison of the cross sections of all Bragg waveguides and their corresponding normalized guided mode profiles at 1560 nm for beam modulation duty cycles of 25% and 50%. For the same modulation duty cycle, waveguides of varying grating orders have cross sections of similar size as a result of delivery of the same average power during fabrication. This is evident for waveguides written with 50% duty cycle, where higher average power and increased deposited energy result in enlarged cross sections and multimode guiding behavior. However, waveguides written with a modulation duty cycle of 25% support only a single guided mode, with a mode field diameter of ~ 8 μm . In addition, no significant deterioration of the mode quality or size is observed over the entire range of Bragg orders written at 25% duty cycle. This suggests that, despite a nominal spot size of 0.765 μm for the writing objective used (0.75 NA), sufficient DC index change due to overlap of the refractive index voxels may be inferred, even for the sixth order Bragg waveguide with a fundamental voxel period of 1.97 μm .

In preparation for spectral measurement, the end facets of the sample were angle ground and polished to reduce back reflections, leaving a final grating length of ~ 20 mm. Broadband emission centered around 1550 nm was coupled into each Bragg waveguide using an angle-cleaved fiber. The reflection spectrum was then collected

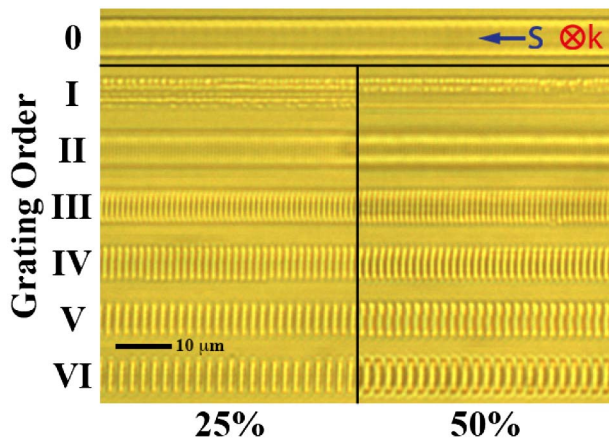


Fig. 1. Top view of laser written Bragg waveguides in GLS ChG glass for 25% and 50% duty cycle. First through sixth order gratings are shown with a zero-order (no grating) waveguide for comparison. All features were written at 300 nJ/pulse, 1 mm/s, and 1.5 ps pulse width. The writing beam was incident into the figure (k), with the writing direction (S) from right to left.

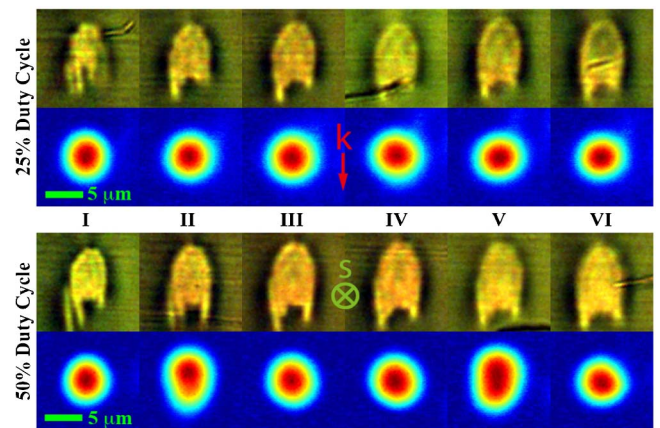


Fig. 2. End facet view of laser-written Bragg waveguides in GLS ChG glass and the corresponding normalized near field profiles at 1560 nm. The writing beam was incident from the top of the figure.

using a circulator inline with the launch fiber, while transmission was collected with a second fiber at the output facet. Finally, both signals were recorded on an optical spectrum analyzer for data analysis. Figure 3 shows the corresponding spectra of a fourth order Bragg waveguide formed with a modulation duty cycle of 25%. The 9.6 dB transmission peak is centered at 1551.02 nm with a narrow bandwidth of 0.09 nm. Broadband radiation mode losses are prominent on the short-wavelength side of the transmission peak, possibly due to scattering. The cross-section images displayed in Fig. 2 show strong evidence of lateral inhomogeneity across the index-modified region. This may be due to macroscopic density variations in the glass as a side effect of the manufacturing process [21]. Furthermore, the grating periods shown in Fig. 1 have a slight curvature, particularly at higher orders. These losses are greatly reduced at higher orders, where coupling is lower and fewer grating periods contribute to losses from scattering [22].

Grating performance is compared between Bragg waveguides of different orders for both 25% and 50% duty cycle, as shown in Fig. 4. The strengths of the transmission peak (dB) and width (FWHM) associated with each Bragg waveguide are plotted versus grating order. As a result of the multimode guiding behavior found in gratings written with 50% duty cycle, multiple resonant wavelength peaks were observed, the strongest of which is used for comparison in Fig. 4. In general, gratings written at 50% duty cycle are weaker than those of the same order written at 25% duty cycle. This is likely due to a reduced fringe visibility as a result of larger overlap between adjacent index voxels.

Most notably, for 25% duty cycle, both the grating strength and width decrease with increasing grating order, which is to be expected, as an increasing multiple of the fundamental period (longer period) results in a lower coupling efficiency for a fixed grating length [22]. Optimal performance is found for Bragg waveguides written with a fourth order period and a duty cycle of 25%, which gives a fair compromise between grating strength and narrow bandwidth.

It is also worthwhile to compare the results shown in Fig. 4 with Bragg waveguides produced by similar

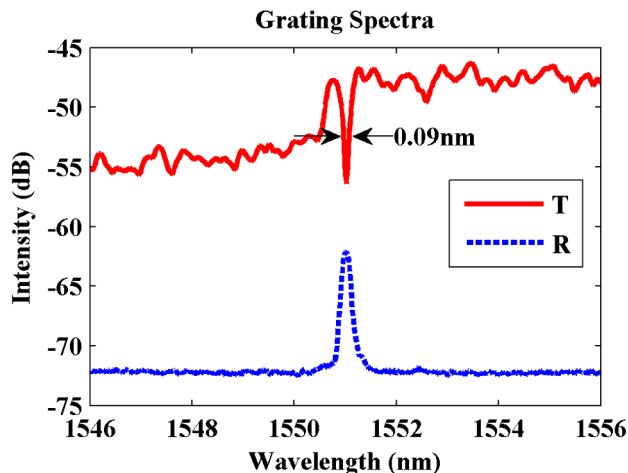


Fig. 3. Transmission and reflection spectra of a fourth order, 20 mm long Bragg waveguide written with 25% duty cycle.

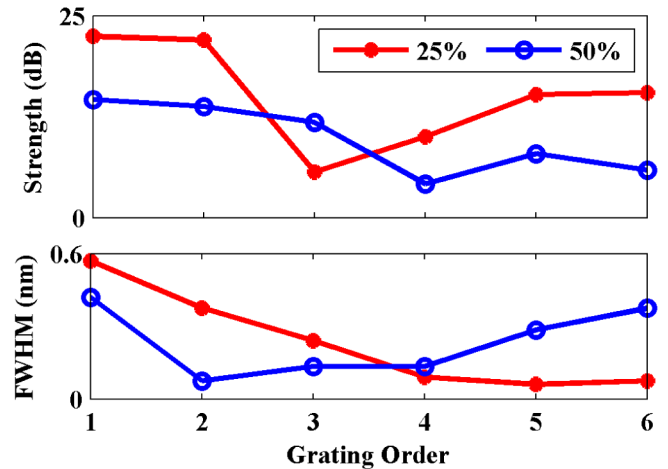


Fig. 4. Strength of the transmission peak and width for first through sixth order Bragg waveguides written with duty cycles of 25% and 50%. The grating length is 20 mm.

fabrication techniques in fused silica. First-order Bragg waveguides with strength of up to 37 dB and a FWHM of 0.3 nm have been reported for a 50-mm-long waveguide in silica using the multiscan technique [14]. Single-scan techniques have also been employed in silica, producing gratings as strong as 35 dB with a FWHM of 0.2 nm for a 28-mm-long waveguide [12]. From these reported grating strengths, the AC index modulations for these two cases are estimated to be 0.31×10^{-4} and 0.58×10^{-4} , respectively. Similar estimates may be inferred for the first-order Bragg waveguides shown in Fig. 4, giving 0.34×10^{-4} and 0.25×10^{-4} for 25% and 50% duty cycles, respectively.

In conclusion, we present laser-written Bragg waveguides in GLS ChG glass with periods from the first through the sixth order. Spatial and temporal beam shaping were employed to control waveguide cross sections and reduce propagation loss. With grating strengths of up to 25 dB, this work enables fabrication of high-quality Bragg waveguides as a fundamental component in nonlinear photonic integrated circuits via the ultrafast laser writing technique.

References

1. A. Zakery and S. R. Elliott, *J. Non-Cryst. Solids* **330**, 1 (2003).
2. C. Quemard, F. Smektala, V. Couderc, A. Barthelemy, and J. Lucas, *J. Phys. Chem. Solids* **62**, 1435 (2001).
3. M. Galili, J. Xu, H. C. Mulvad, L. K. Oxenløwe, A. T. Clausen, P. Jeppesen, B. Luther-Davies, S. Madden, A. Rode, D.-Y. Choi, M. Pelusi, F. Luan, and B. J. Eggleton, *Opt. Express* **17**, 2182 (2009).
4. V. Ta'eed, N. J. Baker, L. Fu, K. Finsterbusch, M. R. E. Lamont, D. J. Moss, H. C. Nguyen, B. J. Eggleton, D.-Y. Choi, S. Madden, and B. Luther-Davies, *Opt. Express* **15**, 9205 (2007).
5. B. J. Eggleton, B. Luther-Davies, and K. Richardson, *Nat. Photonics* **5**, 141 (2011).
6. V. G. Ta'eed, M. Shokooh-Saremi, L. B. Fu, I. C. M. Littler, D. J. Moss, M. Rochette, B. J. Eggleton, Y. L. Ruan, and B. Luther-Davies, *IEEE J. Sel. Top. Quantum Electron.* **12**, 360 (2006).
7. S. J. Madden, D. Y. Choi, D. A. Bulla, A. V. Rode, B. Luther-Davies, V. G. Ta'eed, M. D. Pelusi, and B. J. Eggleton, *Opt. Express* **15**, 14414 (2007).

8. H. C. Nguyen, T. Grujic, K. Finsterbusch, E. C. Magi, F. Libin, B. T. Kuhlmeiy, C. M. de Sterke, and B. J. Eggleton, in *Joint International Conference on Optical Internet, 2007 and the 2007 32nd Australian Conference on Optical Fibre Technology (COIN-ACOFT)* (IEEE, 2007), pp. 1–3.
9. R. R. Gattass and E. Mazur, *Nat. Photonics* **2**, 219 (2008).
10. G. D. Valle, R. Osellame, and P. Laporta, *J. Opt. A* **11**, 013001 (2009).
11. G. D. Marshall, M. Ams, and M. J. Withford, *Opt. Lett.* **31**, 2690 (2006).
12. H. Zhang, S. M. Eaton, and P. R. Herman, *Opt. Lett.* **32**, 2559 (2007).
13. H. Zhang, S. M. Eaton, J. Li, and P. R. Herman, *Opt. Lett.* **31**, 3495 (2006).
14. G. Brown, R. R. Thomson, A. K. Kar, N. D. Psaila, and H. T. Bookey, *Opt. Lett.* **37**, 491 (2012).
15. M. Hughes, W. Yang, and D. Hewak, *Appl. Phys. Lett.* **90**, 131113 (2007).
16. A. M. Weiner, *Rev. Sci. Instrum.* **71**, 1929 (2000).
17. R. Osellame, S. Taccheo, M. Marangoni, R. Ramponi, P. Laporta, D. Polli, S. De Silvestri, and G. Cerullo, *J. Opt. Soc. Am. B* **20**, 1559 (2003).
18. B. McMillen, B. Zhang, K. P. Chen, A. Benayas, and D. Jaque, *Opt. Lett.* **37**, 1418 (2012).
19. R. J. Curry, S. W. Birtwell, A. K. Mairaj, X. Feng, and D. W. Hewak, *J. Non-Cryst. Solids* **351**, 477 (2005).
20. M. Li, S. Huang, Q. Wang, H. Petek, and K. P. Chen, *Opt. Lett.* **39**, 693 (2014).
21. A. B. Seddon, *J. Non-Cryst. Solids* **184**, 44 (1995).
22. T. Erdogan, *J. Lightwave Technol.* **15**, 1277 (1997).